Journal of Ginseng Research 46 (2022) 418–425

Contents lists available at ScienceDirect

Journal of Ginseng Research

journal homepage: https://www.sciencedirect.com/journal/journal-of-ginseng-research

Research Article

Ginsenoside Rg3 in combination with artesunate overcomes sorafenib resistance in hepatoma cell and mouse models

Ying-Jie Chen [a, b, 1], Jia-Ying Wu [a, b, 1], Yu-Yi Deng [a], Ying Wu [a, b], Xiao-Qi Wang [a, b], Amy Sze-man Li [a], Lut Yi Wong [a], Xiu-Qiong Fu [a, b, **], Zhi-Ling Yu [a, b, *], Chun Liang [c, d, ***]

[a] School of Chinese Medicine, Hong Kong Baptist University, China
[b] HKBU Shenzhen Institute for Research and Continuing Education, China
[c] Division of Life Science, Hong Kong University of Science and Technology, China
[d] Enkang Pharmaceuticals (Guangzhou), Ltd., China

ARTICLE INFO

Article history:
Received 20 April 2021
Received in revised form
2 July 2021
Accepted 7 July 2021
Available online 14 July 2021

Keywords:
Artesunate
Ginsenoside Rg3
Hepatoma
Sorafenib resistance
STAT3 signaling

ABSTRACT

Background: Sorafenib is effective in treating hepatoma, but most patients develop resistance to it. STAT3 signaling has been implicated in sorafenib resistance. Artesunate (ART) and 20(R)-ginsenoside Rg3 (Rg3) have anti-hepatoma effects and can inhibit STAT3 signaling in cancer cells. This study aimed to evaluate the effects of Rg3 in combination with ART (Rg3-plus-ART) in overcoming sorafenib resistance, and to examine the involvement of STAT3 signaling in these effects.

Methods: Sorafenib-resistant HepG2 cells (HepG2-SR) were used to evaluate the *in vitro* anti-hepatoma effects of Rg3-plus-ART. A HepG2-SR hepatoma-bearing BALB/c-*nu/nu* mouse model was used to assess the *in vivo* anti-hepatoma effects of Rg3-plus-ART. CCK-8 assays and Annexin V-FITC/PI double staining were used to examine cell proliferation and apoptosis, respectively. Immunoblotting was employed to examine protein levels. ROS generation was examined by measuring DCF-DA fluorescence.

Results: Rg3-plus-ART synergistically reduced viability of, and evoked apoptosis in HepG2-SR cells, and suppressed HepG2-SR tumor growth in mice. Mechanistic studies revealed that Rg3-plus-ART inhibited activation/phosphorylation of Src and STAT3 in HepG2-SR cultures and tumors. The combination also decreased the STAT3 nuclear level and induced ROS production in HepG2-SR cultures. Furthermore, over-activation of STAT3 or removal of ROS diminished the anti-proliferative effects of Rg3-plus-ART, and removal of ROS diminished Rg3-plus-ART's inhibitory effects on STAT3 activation in HepG2-SR cells.

Conclusions: Rg3-plus-ART overcomes sorafenib resistance in experimental models, and inhibition of Src/STAT3 signaling and modulation of ROS/STAT3 signaling contribute to the underlying mechanisms. This study provides a pharmacological basis for developing Rg3-plus-ART into a novel modality for treating sorafenib-resistant hepatoma.

1. Introduction

Hepatoma, also known as hepatocellular carcinoma, is the sixth most common cancer worldwide, with over 906,000 new cases in 2020 (https://gco.iarc.fr/). More threateningly, it is the third leading cause of cancer deaths in the world (https://gco.iarc.fr/). First-line drugs for patients with advanced hepatoma include sorafenib (targeted therapy) and atezolizumab plus bevacizumab (immunotherapy) [1,2]. Owing to its higher cost-effectiveness ratio compared to atezolizumab plus bevacizumab, sorafenib is more widely used [3]. However, sorafenib can only extend the median survival time of hepatoma patients by approximately 3 months, as patients develop resistance to it [4]. Sorafenib resistance in

* Corresponding author. School of Chinese Medicine, Hong Kong Baptist University, Hong Kong.
** Corresponding author. School of Chinese Medicine, Hong Kong Baptist University, Hong Kong.
*** Corresponding author. Division of Life Science, Hong Kong University of Science and Technology, Hong Kong.
E-mail addresses: makyfu@hkbu.edu.hk (X.-Q. Fu), zlyu@hkbu.edu.hk (Z.-L. Yu), bccliang@ust.hk (C. Liang).
[1] These authors contributed equally to this work.

https://doi.org/10.1016/j.jgr.2021.07.002

hepatoma is a complex condition. Several mechanisms underlying sorafenib resistance have been discovered, such as abnormal activation of EGFR (epidermal growth factor receptor) signaling, Raf/MEK/ERK signaling, PI3K/AKT signaling and STAT3 (signal transducer and activator of transcription 3) signaling [5,6]. Activation of these pathways restrains the anti-tumor effects of sorafenib and promotes the proliferation of, and reduces apoptosis in, hepatoma cells. Two multi-targeted tyrosine kinase inhibitors, regorafenib and cabozantinib, and a VEGFR2 inhibitor, ramucirumab, have been approved as second-line treatments for patients with sorafenib-resistant hepatoma. Unfortunately, like sorafenib, they failed to show durable therapeutic responses [7]. Novel agents for treating sorafenib-resistant hepatoma are needed.

20(R)-Ginsenoside Rg3 (Rg3) is a main bioactive triterpenoid saponin of red ginseng (steamed roots and rhizomes of *Panax ginseng*). It has been approved as an adjuvant drug, named Shenyi Capsule, for cancer management in China [8]. Clinical studies showed that Rg3 enhances the efficacy and reduces the toxicities of conventional anti-cancer drugs. For instance, Rg3 can reduce the side effects of anlotinib, and can improve the life quality of anlotinib-treated patients with non-small cell lung cancer [9]. Tan et al demonstrated that combined treatment with Rg3 and Docetaxel achieved better outcomes in advanced gastric cancer patients than Docetaxel mono-treatment [10]. Laboratory studies showed that Rg3 inhibits tumor angiogenesis [11], and suppresses multiple oncogenic pathways to exert cytotoxic effects against cancer cells [12]. Rg3 has also been shown to be able to overcome multi-drug resistance (MDR) in cancer cells [13].

Artesunate (ART), an approved antimalarial drug, is a derivative of artemisinin, a sesquiterpene lactone found in the medicinal herb *Artemisia annua* L [14]. ART contains an endoperoxide moiety that can react with intracellular free iron to kill cancer cells by generating cytotoxic free radicals [15]. The anti-cancer feasibility of ART has been validated by clinical studies. Krishna et al found that oral administration of ART increases the recurrence-free survival of patients with colorectal cancer [16]. Another clinical trial showed that ART is effective in treating patients with metastatic breast cancer [17]. Recently, ART was found to be able to overcome sorafenib resistance in hepatoma cells [18].

Rg3 and ART have been shown to inhibit STAT3 signaling [11,19]. Xu et al found that co-administration of Rg3 and ART can inhibit tumor growth in an S180 sarcoma mouse model [20]. Whether the combination of Rg3 and ART (Rg3-plus-ART) overcomes sorafenib resistance in hepatoma is unknown. Objectives of this study were to evaluate the effects of Rg3-plus-ART in overcoming sorafenib resistance in hepatoma, and to examine the involvement of STAT3 signaling in these effects.

2. Materials and methods

2.1. Reagents

Rg3 and ART (purity > 98%, determined by HPLC) were purchased from Plant Origin Biological (Nanjing, China). Chemical structures of Rg3 and ART are shown in Fig. 1A and B, respectively. Brivanib (purity > 98%, determined by HPLC) was obtained from Yuanye Bio-Technology Co. (Shanghai, China). Stattic (a specific STAT3 inhibitor) and N-acetylcysteine (NAC) were obtained from Sigma Chemical Co. (USA). CCK-8 (Cell Counting Kit-8) was purchased from TransGen Biotech (Beijing, China). Monoclonal antibodies of Src, phospho-Src (Tyr416), STAT3, phospho-STAT3 (Tyr705), Bcl-2, Mcl-1, cleaved-Poly (ADP-ribose) polymerase (PARP) were purchased from Cell Signaling Technology (USA). Monoclonal antibodies of β-actin and lamin B1 were purchased from Santa Cruz Biotechnology (USA). Dulbecco's modified eagle medium (DMEM), penicillin/streptomycin (P/S) and fetal bovine serum (FBS) were obtained from GIBCO (Gaithersburg, MD, USA).

2.2. Cell culture

HepG2-SR cells were generated as previously described with some modifications [21]. Briefly, parental HepG2 human hepatoma cells (purchased from ATCC) were cultured in DMEM with 5% FBS and increasing concentrations of sorafenib (0.1–5 μM) for 3 months and then maintained in 5 μM sorafenib thereafter. After that, HepG2-SR cells were cultured in DMEM containing 1% P/S and 10% FBS in a humidified atmosphere of 5% CO_2 at 37°C for different durations in different experiments.

2.3. Cell viability assay

A CCK-8 assay kit was employed to determine the effects of Rg3, ART and Rg3-plus-ART on the viability of HepG2-SR cells following the kit manufacturer's protocol. Cells were seeded in 96-well plates (3,000 cells/well or 1,500 cells/well) overnight and treated with Rg3 (50, 75 μM), ART (10, 15 μM), Rg3-plus-ART (50 μM + 10 μM, 75 μM + 15 μM) or brivanib (2.5, 5 μM) for 48 hrs/72 hrs. Then, 20 μl of CCK-8 solution was added into each well and incubated for 4 hrs. Absorbance of each well was measured at 450 nm with a microplate spectrophotometer (BD Biosciences, USA). Doses of Rg3 and ART were set based on previous reports. It has been reported that 50 μM Rg3 [22] and 10 μM ART [23] were able to suppress proliferation of HepG2 cells.

Synergism of the drug combination was evaluated using the coefficient of drug interaction (CDI) value. CDI value was calculated by the equation CDI = AB/(A × B). According to the absorbance value of each group, AB is the ratio of the combination group to the vehicle group; A or B is the ratio of individual mono-treatment group to the vehicle group. CDI < 1 shows a synergistic effect, while CDI <0.7 shows a significant synergistic effect.

2.4. Apoptosis assay

Apoptotic effects of Rg3-plus-ART on HepG2-SR cells were measured by Annexin V-FITC/PI double staining using an Apoptosis Detection Kit (#ab14085; Abcam) following the kit manufacturer's protocol. HepG2-SR cells were seeded in 6-well plates (1×10^5cells/well) and treated with various concentrations of Rg3, ART, Rg3-plus-ART or brivanib for 24 hrs/48 hrs. A BD Accuri C6 flow cytometer (BD Biosciences, USA). was used to perform the flow cytometric analyses.

2.5. Animal experiments

Male 7-week-old BALB/c-*nu/nu* mice (body weight: 20 ± 2 g) were purchased from The Chinese University of Hong Kong. Animal care and handling performances were approved by the Department of Health, Hong Kong (DH/HT&A/8/2/6 Pt. 1). Mice were housed in the animal facility of Hong Kong Baptist University (temperature: 25 ± 2 °C; humidity: 60 ± 10%; 12-hr light/dark cycle) and were fed with water and standard rodent pellets. Before the experiments, mice were acclimatized for one week.

HepG2-SR cells (1×10^7) in PBS were mixed with Matrigel at the ratio of 1:1, and s.c. injected into the flank of individual BALB/c-*nu/nu* mice (0.2 ml each). After growing for 5 days, 24 mice were randomly divided into four groups with 6 mice in each group. Mice were daily i.g. administered with vehicle (PBS solution containing 5% Tween 80 and 5% PEG400, model group), 6 mg/kg Rg3 + 7.5 mg/kg ART (low dose group), 12 mg/kg Rg3 + 15 mg/kg ART (high dose group) or 100 mg/kg brivanib (positive control group) for 15

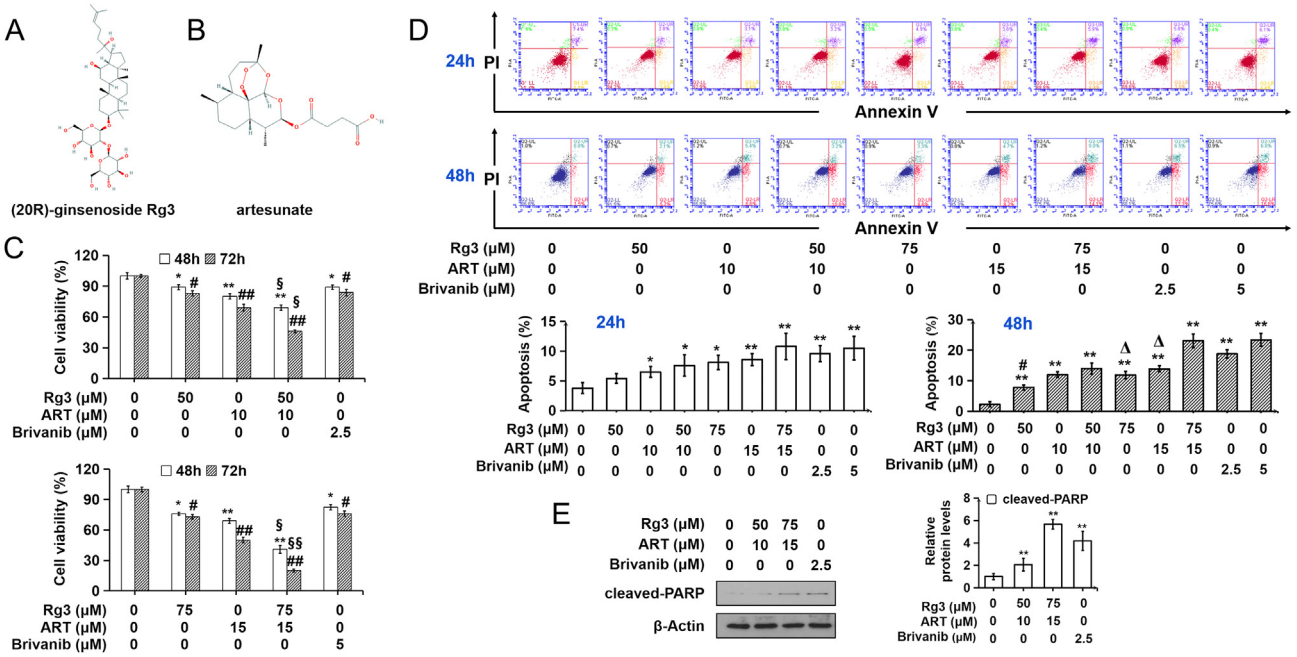

Fig. 1. Rg3-plus-ART reduces viability of, and induced apoptosis in HepG2-SR cells. **(A) - (B)** Chemical structures of Rg3 and ART. **(C)** Viability of HepG2-SR cells. The viability of solvent-treated cells was regarded as 100%. Data from three independent experiments are presented as mean ± SD. *$P < 0.05$, **$P < 0.01$ *vs.* the solvent-treated (48 hrs) group; #$P < 0.05$, ##$P < 0.01$ *vs.* the solvent-treated (72 hrs) group. § CDI <1, §§ CDI <0.7. **(D)** Rg3-plus-ART induces apoptosis in HepG2-SR cells. Representative scatter graphs are shown in the upper panels. FITC positive cells (the right quadrants) are regarded as apoptotic cells. Quantitative results are shown in the lower panel. Data from three independent experiments are presented as mean ± SD. *$P < 0.05$, **$P < 0.01$ *vs.* the solvent-treated group; #$P < 0.05$ *vs.* the 50 μM Rg3 + 10 μM ART-treated group; Δ $P < 0.05$ *vs.* the 75 μM Rg3 + 15 μM ART-treated group. **(E)** Protein levels of cleaved-PARP in HepG2-SR cultures. Cells were treated with indicated concentrations of Rg3-plus-ART for 48 hrs. β-Actin served as a loading control. Representative immunoblotting results are shown in the left panel, and quantitative results are shown in the right panel. Data are expressed as mean ± SD of 3 independent experiments. *$P < 0.05$, **$P < 0.01$ *vs.* the solvent-treated group. In **(C)** - **(E)**, brivanib was used as positive control.

consecutive days. Doses of Rg3 and ART were set based on human equivalents. The 6 mg/kg dose of Rg3 is its human equivalent dose for treating cancer [8]. The 15 mg/kg dose of ART is its human equivalent dose for treating malaria [24]. To investigate the inhibitory effects of Rg3-plus-ART on tumor growth, tumor volumes were measured with a Vernier caliper every 3 days.

To monitor potential toxicities of Rg3-plus-ART in mice, general clinical observations, such as changes in skin, fur, eyes, secretions, excretions, autonomic activities, gait, posture and response to handling, were performed once a day [25]. Body weight and food intake of mice were recorded every 3 days. Mice were executed with excessive anesthesia (isoflurane, 5%) at the end of the experiments. The tumor and main organs (heart, lung, spleen, kidney, and liver) of each mouse were quickly removed and weighed. Gross necropsy was performed for all the dissected organs and tissues.

2.6. Immunoblotting

Lysates were prepared from HepG2-SR tumors and cultured HepG2-SR cells as previously described [26]. Briefly, each tumor was homogenized in RIPA lysis buffer [50 mM Tris-HCl, 1% NP-40, 0.35% sodium-deoxycholate, 150 mM NaCl, 1 mM EDTA (pH 7.4), 1 mM phenylmethylsulfonyl fluoride, 1 mM NaF, 1 mM Na_3VO_4, and 10 μg/mL each of aprotinin, leupetin and pepstatin A]. After incubation on ice for 15 min, the homogenate was centrifuged at 14,000 g for 30 min at 4 °C, and the supernatant was collected as a protein sample. For whole-cell protein preparations, HepG2-SR cells were lysed in RIPA lysis buffer for 15 min on ice. Then the lysates were centrifuged at 14,000 g at 4 °C for 15 min, and the supernatants were collected. Extracts of cytoplasm and cell nucleus were prepared using the Mammalian Nuclear and Cytoplasmic Protein Extraction Kit (TransGen Biotech, Beijing, China) following the manufacturer's protocol. A Quick Start™ Bradford Protein Assay (Bio-Rad, USA) was used to measure protein concentrations. Each protein sample was mixed with 5-times volume of loading dye (Laemmli Buffer) containing 1% 2-mercaptoethanol, and was heated at 95 °C for 5 min [27].

Western blot assays were performed as previously described [27]. Briefly, equal amounts of protein were subjected to 10% sodium dodecyl sulfate-polyacrylamide gel electrophoresis. The proteins were electro-transferred from the gel onto a nitrocellulose membrane for 150 min under 350 mA. The membrane was blocked with 5% non-fat milk in Tris-buffered saline (150 mM NaCl, 20 mM Tris—HCl, pH 7.4) with 0.05% Tween 20 buffer (TBST) for 1 hr at room temperature. After blocking, the membrane was incubated with primary antibodies in 2.5% non-fat milk-TBST solution overnight at 4 °C. The membrane was then washed with TBST solution and incubated with an anti-mouse or anti-rabbit secondary antibody for 1 hr. To investigate the effects of Rg3-plus-ART on STAT3 signaling, monoclonal antibodies of Src, phospho-Src (Tyr416), STAT3, phospho-STAT3 (Tyr705), Bcl-2 and Mcl-1 were used. To monitor apoptosis, cleaved-PARP, an apoptotic marker, was detected using a specific monoclonal antibody.

Immunoreactive bands were visualized using the Enhanced Chemiluminescence Detection Kit (Invitrogen, USA). Intensity of each band was measured using Image J (http://rsb.info.nih.gov/ij/). In brief, high resolution images of immunoreactive bands were imported to Image J and converted to 8-bit format. The “Subtract Background” tool was used to smoothe the images. As the software measures the gray values of the 8-bit images, the image color was inverted using the “Invert” function in the edit menu. Finally, individual bands were selected using the “Freehand Selection” tool, and the value of intensity of each band was obtained from the “Measure” function under the menu of “Analysis”. The relative level

of a protein of interest was normalized to the endogenous β-actin or lamin B1 value.

2.7. Measurement of reactive oxygen species (ROS)

HepG2-SR cells seeded in black 96-well plates (3,000 cells/well) overnight were treated with a fluorescent dye (10 μM DCF-DA; 6-Carboxy-2′,7′-dichlorofluorescein diacetate) for 45 min. The supernatant was then discarded and replaced with fresh medium. Afterwards, the cells were treated with 75 μM Rg3, 15 μM ART or 75 μM Rg3 + 15 μM ART. Fluorescence was measured using a fluorescence microplate reader (EnVision® Multilabel Reader, PerkinElmer) at various time points at 37 °C [26]. For DCF-DA fluorescence microscopic analyses, HepG2-SR cells seeded in 6-well plate (1×10^5cells/well) were treated with 75 μM Rg3 + 15 μM ART and/or 5 mM NAC for 8 hrs. The cells were then treated with 10 μM DCF-DA for 45 min. Afterwards, samples were rinsed three times with PBS, and then counter-stained with DAPI [26]. Images were obtained by a Leica DMI3000 B microscope (Leica Microsystems, Wetzlar, Germany).

2.8. Cell transient transduction

STAT3C (A662C, N664C mutant) is a constitutively active STAT3 variant. Adenovirus expressing GFP (green fluorescent protein)-Flag-tagged STAT3C (Ad-STAT3C) and control adenovirus expressing GFP (Ad-Empty vector) were purchased from Vigene Biosciences (Shandong, China). HepG2-SR cells (6×10^5 cells/dish) were seeded in 100 mm dishes and transduced with Ad-STAT3C (7.8×10^6 pfu/ml, HepG2-SR^{STAT3C}) or Ad-Empty vector (7.8×10^6 pfu/ml, HepG2-SR$^{Empty\ vector}$) for 24 hrs, after which the supernatants were discarded and replaced with fresh media. After 12 hrs, transduced HepG2-SR cells: HepG2-SR$^{Empty\ vector}$ and HepG2-SR^{STAT3C} were used for experiments [28].

2.9. Statistical analysis

Data are presented as the means ± standard deviation (SD). Comparison of quantitative data in multiple groups was performed using one-way analysis of variance (ANOVA) followed by Tukey's test using the statistical software GraphPad Prism 6.0 (GraphPad Software, San Diego, CA, USA). $P < 0.05$ was regarded as statistically significant.

3. Results

3.1. Rg3-plus-ART reduces viability of, and induces apoptosis in HepG2-SR cells

A CCK-8 assay kit was employed to evaluate the respective effects of Rg3, ART and Rg3-plus-ART on HepG2-SR cell proliferation. Results showed that treatments with Rg3 (50, 75 μM), ART (10, 15 μM), or Rg3-plus-ART (50 μM Rg3 + 10 μM ART, 75 μM Rg3 + 15 μM ART) for 48 hrs or 72 hrs reduced the viability of HepG2-SR cells in time- and dose-dependent manners (Fig. 1C). CDI value was calculated to evaluate the synergism of Rg3 and ART. For 48-hr treatments, the CDI values of 50 μM Rg3 plus 10 μM ART, and 75 μM Rg3 plus 15 μM ART were 0.969 and 0.803, respectively. For 72-hr treatments, the CDI values of the two combination groups were 0.782 and 0.685, respectively. It was found that 50 μM Rg3 plus 10 μM ART in 48-hr treatment and 72-hr treatment assays, and 75 μM Rg3 plus 15 μM ART in the 48-hr treatment assay exerted synergistic effects (CDI<1); and that 75 μM Rg3 plus 15 μM ART in the 72-hr treatment assay exerted significant synergistic effects (CDI<0.7) in inhibiting HepG2-SR cell proliferation.

Respective pro-apoptotic effects of Rg3, ART and Rg3-plus-ART on HepG2-SR cells were examined using flow cytometric analyses after Annexin V-FITC/PI double staining. Results showed that Rg3, ART or Rg3-plus-ART induced cell apoptosis in dose- and time-dependent manners (Fig. 1D). After a 24-hr treatment, apoptosis rates in the control group, 50 μM Rg3 group, 10 μM ART group, 50 μM Rg3 + 10 μM ART group, 75 μM Rg3 group, 15 μM ART group and 75 μM Rg3 + 15 μM ART group were 3.8 ± 0.9 %, 5.4 ± 0.8 %, 6.5 ± 0.9 %, 7.6 ± 1.8 %, 8.1 ± 1.2 %, 8.6 ± 1.0 % and 10.8 ± 2.2%, respectively. After a 48-hr treatment, apoptosis rates in these groups were 2.3 ± 0.8 %, 7.8 ± 1.3 %, 12.0 ± 1.9 %, 14.0 ± 3.2 %, 11.9 ± 1.7 %, 13.9 ± 2.8 % and 23.1 ± 4.8 %, respectively. Further analysis of these obtained data revealed that combined treatments exerted stronger pro-apoptotic effects than mono-treatments (Fig. 1D). Western blotting results showed that the drug combination dose-dependently elevated the protein level of cleaved PARP, an apoptotic marker, confirming the apoptotic effects of the combination (Fig. 1E). Brivanib, a VEGFR inhibitor that is able to overcome sorafenib resistance in hepatoma cell and animal models [29], was used as a positive control. It reduced the viability of, and induced apoptosis in, HepG2-SR cells as expected. These findings indicate that Rg3-plus-ART reduces the viability of, and induces apoptosis in, HepG2-SR cells.

3.2. Rg3-plus-ART suppresses HepG2-SR hepatoma growth in mice

A BALB/c-*nu/nu* nude mouse HepG2-SR xenograft model was used to evaluate the *in vivo* anti-hepatoma effects of Rg3-plus-ART. As shown in Fig. 2A, intragastric (i.g.) treatment with 6 mg/kg Rg3 + 7.5 mg/kg ART, 12 mg/kg Rg3 + 15 mg/kg ART, or 100 mg/kg brivanib daily for 15 consecutive days inhibited HepG2-SR hepatoma growth in mice. Fig. 2B showed that the average tumor weights in the two Rg3-plus-ART groups and the positive control group were significantly lower than that in the model group at the end of the experiment. From day 12 to day 15 after dosing, the combination significantly suppressed tumor growth in dose- and time-dependent manners. The positive control drug brivanib also significantly inhibited tumor growth from day 12 after dosing (Fig. 2C).

Rg3-plus-ART and brivanib had no obvious influence on mouse body weight (Fig. 2D). No mouse death was observed during the experiment. No abnormalities at necropsy or in clinical signs, and no significant differences in food consumption were observed (data not shown). These results indicate that the treatments inhibited tumor growth without significant toxicities in the sorafenib-resistant hepatoma mouse model.

3.3. Inhibition of Src/STAT3 signaling contributes to Rg3-plus-ART's effects in overcoming sorafenib resistance in hepatoma models

Activation of STAT3 signaling has been reported to promote sorafenib resistance in hepatoma [30]. Immunoblotting was performed to examine the effects of Rg3-plus-ART on STAT3 signaling. Results showed that both the low and high doses of Rg3-plus-ART significantly down-regulated the protein level of phospho-Src (Tyr416, an up-stream kinase of STAT3), and the high dose of Rg3-plus-ART significantly down-regulated the protein level of phospho-STAT3 (Tyr705) in HepG2-SR tumors (Fig. 3A). Rg3-plus-ART did not affect the levels of Src and STAT3 in tumor tissues (Fig. 3A). The positive control drug brivanib also significantly inhibited the phosphorylation of Src and STAT3 in tumor tissues (Fig. 3A).

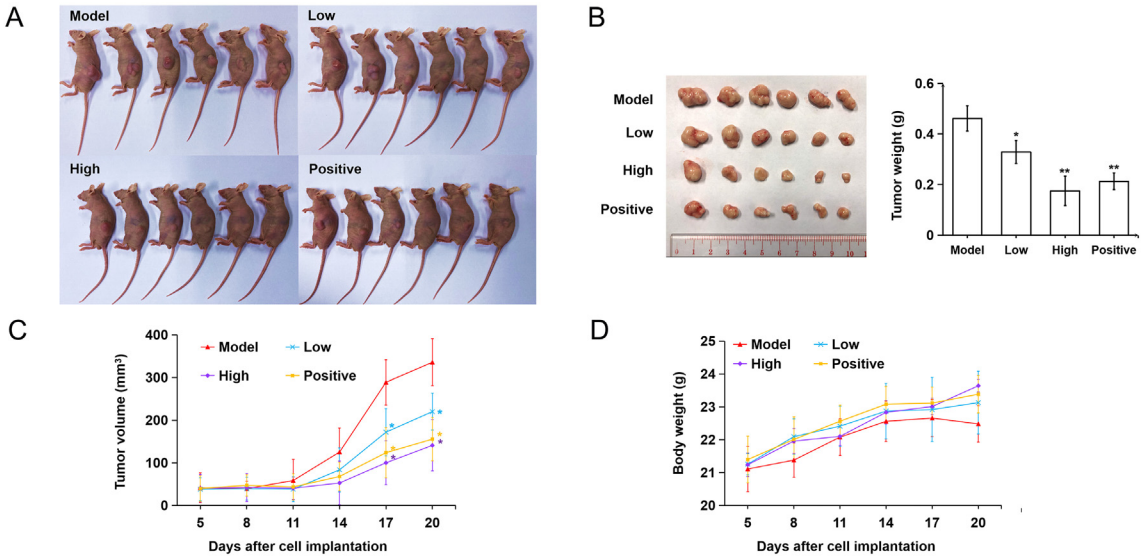

Fig. 2. Rg3-plus-ART suppresses HepG2-SR tumor growth in mice. **(A)** Images of mice after drug administration. **(B)** Tumor weights of mice at the end of the experiment. Representative images of tumors (the left panel) and weights of tumors (the right panel) are shown. **(C)** Tumor volumes. Tumor volumes of each mouse were measured at the indicated time points. **(D)** Body weights of mice at the indicated time points. Data are expressed as mean ± SD (n = 6). $*P < 0.05$, $**P < 0.01$ *vs.* the model group.

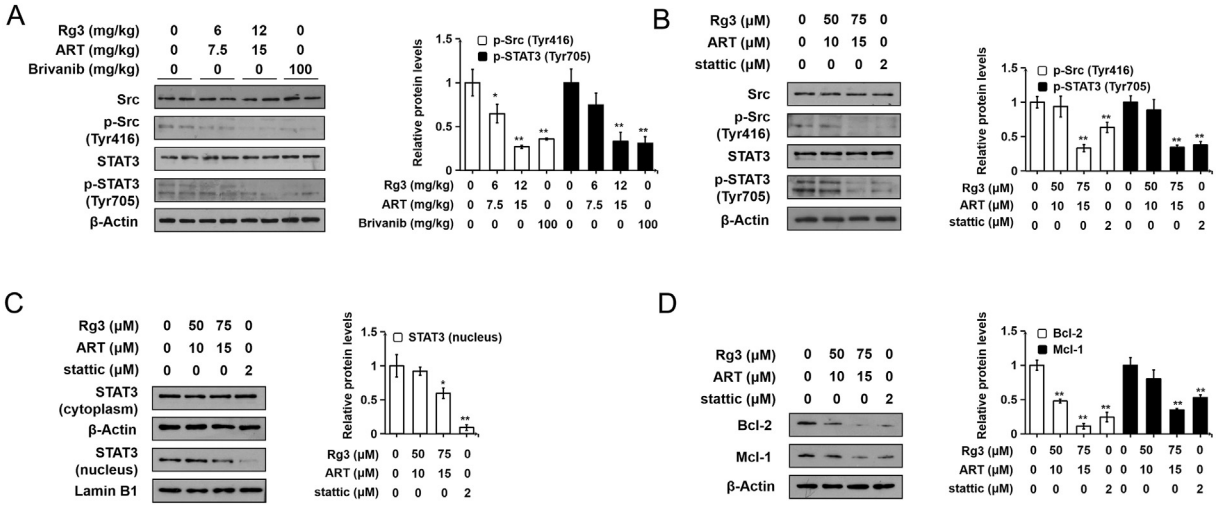

Fig. 3. Rg3-plus-ART inhibits the Src/STAT3 pathway in tumor tissues and in cultured HepG2-SR cells. **(A)** Protein levels of phospho-Src (Tyr416), phospho-STAT3 (Tyr705), Src and STAT3 in tumor tissues of mice. Data are expressed as mean ± SD (n = 6) $*P < 0.05$, $**P < 0.01$ *vs.* the model group. **(B)** Protein levels of phospho-Src (Tyr416), phospho-STAT3 (Tyr705), Src and STAT3 in HepG2-SR cultures. **(C)** Protein levels of Bcl-2 and Mcl-1 in HepG2-SR cultures. In **(B)** and **(C)**, cells were incubated with the indicated concentrations of Rg3-plus-ART or stattic for 24 hrs. In **(A)** - **(C)**, β-actin served as the loading control. **(D)** Protein levels of STAT3 in cytoplasm and nuclear extracts. Lamin B1 and β-actin served as the loading controls of nuclear and cytoplasmic extracts, respectively. Cells were incubated with the indicated concentrations of Rg3-plus-ART or stattic for 30 min. Representative immunoblotting results are shown in the left panel, and quantitative results are shown in the right panel. In **(B)** - **(D)**, Data are expressed as mean ± SD of 3 independent experiments. $*P < 0.05$, $**P < 0.01$ *vs.* the solvent-treated group.

In HepG2-SR cultures, the high dose of Rg3-plus-ART down-regulated protein levels of phospho-Src (Tyr416) and phospho-STAT3 (Tyr705) without affecting the levels of Src and STAT3 (Fig. 3B). The high dose of Rg3-plus-ART also significantly decreased the nuclear STAT3 level (Fig. 3C). Rg3-plus-ART dose-dependently and significantly down-regulated the protein level of Bcl-2, and the high dose of the combination significantly lowered Mcl-1 protein level. Both Bcl-2 and Mcl-1 are STAT3 target genes involved in cell survival. Stattic, a specific STAT3 inhibitor, was used as a positive control; and it inhibited STAT3 signaling in HepG2-SR cultures as well (Fig. 3B–D).

The above findings indicate that Rg3-plus-ART inhibits Src/STAT3 signaling in mouse HepG2-SR tumors and in HepG2-SR cells.

To determine whether Src/STAT3 signaling contributed to the inhibitory effects of Rg3-plus-ART on the viability of HepG2-SR cells, we over-activated STAT3 in HepG2-SR cells by transducing a STAT3C plasmid into the cells. Green fluorescent and bright-field microscopy images of the HepG2-SR cells showed that the transduction was successful (Fig. 4A). Transduction of the STAT3C plasmid resulted in a significant elevation of phospho-STAT3 (Tyr705) level compared to transduction with the empty vector (Fig. 4A), showing an overactivation of STAT3 in HepG2-SR cells. Upon STAT3 overactivation, the inhibitory effects of the low and high doses of Rg3-plus-ART on the viability of HepG2-SR cells decreased by 12% and 31%, respectively (Fig. 4B). These results

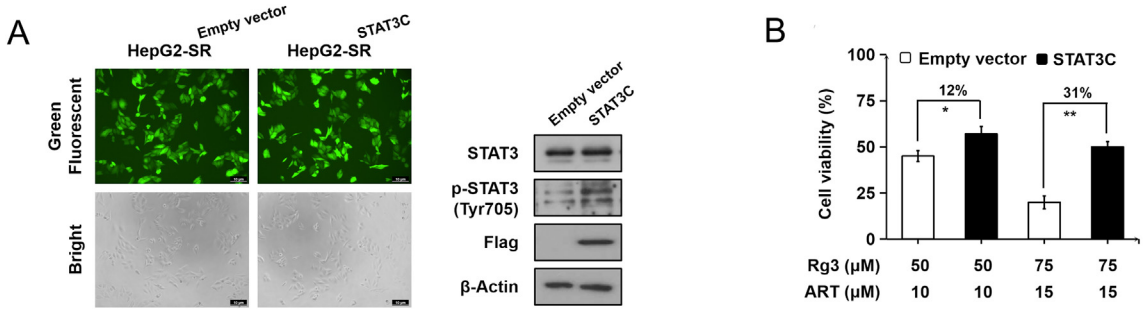

Fig. 4. Over-activation of STAT3 diminishes the inhibitory effects of Rg3-plus-ART on cell viability in HepG2-SR cells. HepG2-SR cells were transduced with the Ad-Empty vector (HepG2-SR$^{\text{Empty vector}}$) or the Ad-STAT3C plasmid (HepG2-SR$^{\text{STAT3C}}$). **(A)** GFP expression and the protein levels of STAT3, phospho-STAT3 (Tyr 705) and Flag in HepG2-SR$^{\text{Empty vector}}$ and HepG2-SR$^{\text{STAT3C}}$ cells. Representative green fluorescent and bright-field microscopy images of HepG2-SR$^{\text{Empty vector}}$ and HepG2-SR$^{\text{STAT3C}}$ (the left panel, scale bar, 10 μm), and representative immunoblotting results (the right panel) are shown. **(B)** Over-activation of STAT3 diminishes the anti-proliferative effects of Rg3-plus-ART in HepG2-SR cells. Differences of relative cell viabilities between Rg3-plus-ART-treated HepG2-SR$^{\text{Empty vector}}$ cells and Rg3-plus-ART-treated HepG2-SR$^{\text{STAT3C}}$ cells were calculated (n = 3). $^{*}P < 0.05$, $^{**}P < 0.01$.

indicate that suppression of STAT3 signaling contributes to Rg3-plus-ART's inhibitory effects on the viability of HepG2-SR cells.

3.4. Induction of ROS production contributes to Rg3-plus-ART's inhibitory effects on cell viability and STAT3 activation in HepG2-SR cultures

It has been reported that enhancing ROS production is a strategy to reverse sorafenib resistance [31]. ROS generation induced by Rg3, ART or Rg3-plus-ART was detected by measuring DCF-DA fluorescence. Results showed that Rg3, ART and Rg3-plus-ART significantly increased ROS production in HepG2-SR cultures in a time-dependent manner (Fig. 5A). The drug combination was more potent than Rg3 or ART alone (Fig. 5A). To determine the contribution of ROS in Rg3-plus-ART's inhibitory effects on the viability of HepG2-SR cells, whether NAC, a ROS scavenger, was able to rescue Rg3-plus-ART-induced cell death, was tested. As shown in Fig. 5B, Rg3-plus-ART-induced ROS generation indicated by green

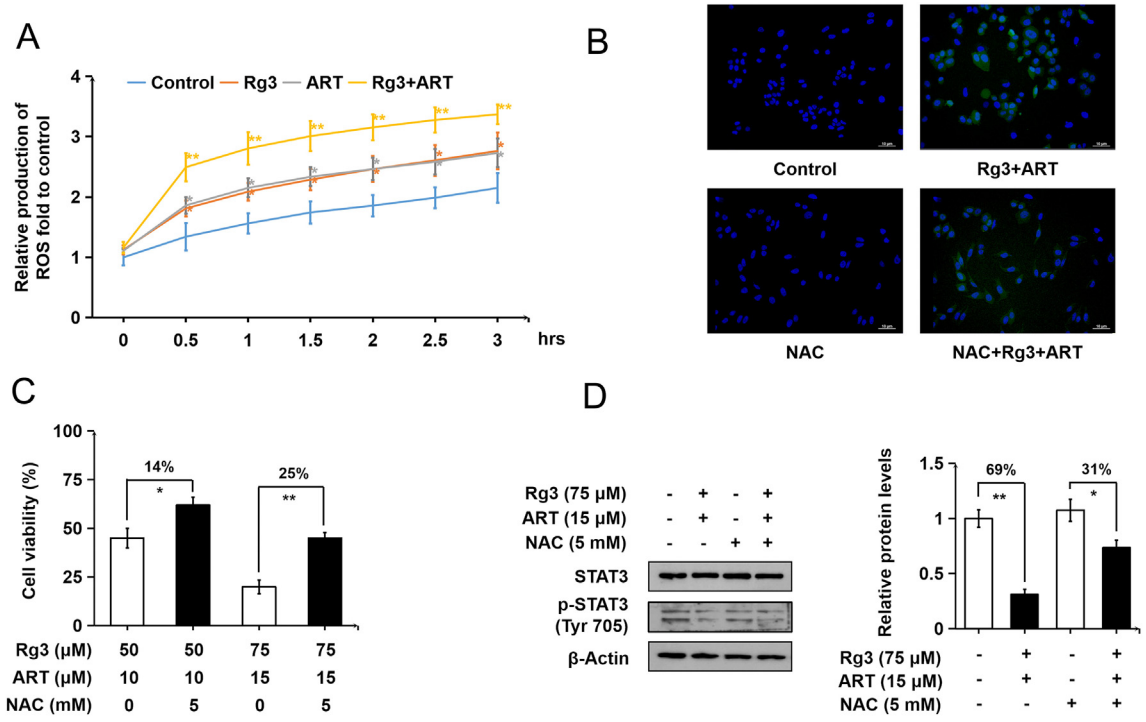

Fig. 5. Induction of ROS production contributes to Rg3-plus-ART's inhibitory effects on cell viability and STAT3 activation in HepG2-SR cultures. (A) Rg3, ART and Rg3-plus-ART induced ROS production in HepG2-SR cells. Relative ROS production in the control group at 0 hr was regarded as 1. Data are expressed as mean ± SD of 3 independent experiments. $^{*}P < 0.05$, $^{**}P < 0.01$ *vs.* the solvent-treated control group. **(B)** Fluorescence microscopy images of DAPI- and DCF-DA-stained HepG2-SR cells treated with Rg3-plus-ART and/or NAC for 8 hrs. ROS generated in cells displayed green fluorescence, and cell nuclei displayed blue fluorescence. Scale bar, 10 μm. **(C)** Co-treatment with NAC diminishes Rg3-plus-ART's inhibitory effects on the viability of HepG2-SR cells. Cells were treated with indicated concentrations of Rg3-plus-ART with or without 5 mM NAC for 72 hrs. Differences in the relative cell viabilities between the NAC-treated group and NAC-untreated group were calculated. Data from three independent experiments are presented as mean ± SD. $^{*}P < 0.05$, $^{**}P < 0.01$. **(D)** NAC diminishes the inhibitory effects of Rg3-plus-ART on STAT3 phosphorylation in HepG2-SR cultures. Cells were treated with 75 μM Rg3 + 15 μM ART and/or 5 mM NAC for 24 hrs. Representative immunoblotting results are shown in the left panel, and quantitative results are shown in the right panel. Differences in the relative protein levels of phospho-STAT3 (Tyr705) between the Rg3-plus-ART-treated group and Rg3-plus-ART-untreated group were calculated. Data are expressed as mean ± SD of 3 independent experiments. $^{*}P < 0.05$, $^{**}P < 0.01$.

fluorescence in HepG2-SR cells, and NAC decreased Rg3-plus-ART-induced ROS production. Fig. 5C showed that scavenging ROS diminished the inhibitory effects of the low and high doses of Rg3-plus-ART on the viability of HepG2-SR cells by 14% and 25%, respectively. These results indicate that ROS production induced by Rg3-plus-ART contributes to the inhibitory effects of the drug combination on HepG2-SR cell viability.

It has been reported that ROS inactivates STAT3 in drug-resistant cancer cells [32,33]. We investigated if Rg3-plus-ART inhibited STAT3 activation/phosphorylation by inducing ROS production in HepG2-SR cells. In this regard, NAC was used to scavenge ROS. Western blotting results showed that Rg3-plus-ART decreased the protein levels of phospho-STAT3 (Tyr 705) in NAC-untreated and NAC-treated cultures by 69% and 31%, respectively (Fig. 5D), indicating that NAC decreased the inhibitory effects of Rg3-plus-ART on STAT3 phosphorylation by 38% (Fig. 5D). These results indicate that induction of ROS contributes to the inhibitory effects of Rg3-plus-ART on STAT3 activation in HepG2-SR cells.

4. Discussion

Natural compounds have been recognized as a resource for anticancer drug discovery. One of the major mechanisms underlying the resistance of cancers to targeted drugs is the activation of complex compensatory signaling pathways [34]. Owing to the multi-target nature of natural compounds, they have advantages in managing complex conditions. However, this property may also be a cause for low drug efficacy. Combined treatments with natural compounds may have higher efficacies than mono-compound treatments. Many combinations of natural compounds have been shown to be able to overcome cancer drug resistance. For example, the combination of resveratrol and paclitaxel can reverse MDR in a breast cancer mouse model [35]. Zou et al found that paclitaxel in combination with borneol can overcome paclitaxel-resistance in ovarian cancer cell and animal models [36]. However, none of these combinations have been approved for clinical use. Recently, drug repurposing has attracted tremendous interest as a strategy for discovering new therapeutics for malignant diseases [37]. Repurposing old drugs has advantages compared to the development of new entities, as old drugs' toxicities and pharmacokinetics profiles are already well-studied in human beings [38]. In the present study, it was found that Rg3-plus-ART is able to overcome sorafenib resistance in hepatoma. Both Rg3 and ART are approved clinical drugs, so Rg3-plus-ART has good potential to be developed into an adjuvant drug for treating sorafenib-resistant hepatoma.

The STAT3 signaling pathway has been linked to the development of sorafenib resistance. In sorafenib-resistant hepatoma cells, STAT3 is activated by its up-stream kinases such as Src. Activated STAT3 forms homodimers and then translocates to the nucleus to regulate the transcription of its target genes, e.g. cell survival-related genes Bcl-2 and Mcl-1 [39]. Inhibiting STAT3 can induce apoptosis in sorafenib-resistant hepatoma cells [40]. Therefore, STAT3 has been regarded as a target for overcoming sorafenib resistance. In the present study, Rg3-plus-ART inhibited phosphorylation of STAT3 and its up-stream kinase Src, lowered the nuclear STAT3 level, and down-regulated protein levels of Mcl-1 and Bcl-2 in HepG2-SR cells. Moreover, over-activation of STAT3 in HepG2-SR cells diminished Rg3-plus-ART's cytotoxic effects. These results indicate that inhibition of Src/STAT3 signaling is a mechanism underlying Rg3-plus-ART's effects in overcoming sorafenib resistance in hepatoma.

In addition to promote sorafenib resistance in hepatoma, STAT3 signaling plays a central role in the development and progression of hepatoma [1]. It is warranted to examine whether Rg3-plus-ART has anticancer effects in previously untreated hepatoma in future studies.

Drug-induced ROS can kill cancer cells [41]. Sorafenib-resistant hepatoma cells have reduced ROS levels [31]. Enhancing ROS production has been shown to be able to overcome sorafenib resistance in hepatoma [31]. In this study, it was found that Rg3-plus-ART promotes ROS production, and scavenging ROS diminishes Rg3-plus-ART's inhibitory effects on viability and STAT3 activation in HepG2-SR cells. These results indicate that inducting ROS production to inactivate STAT3 contributes to Rg3-plus-ART's effects in overcoming sorafenib resistance in hepatoma.

The EGFR/PI3K/AKT pathway and the Raf/MEK/ERK pathway are also involved in sorafenib resistance in hepatoma [5]. Both Rg3 and ART can inhibit these pathways in cancer cells [42–45]. Whether these two pathways are involved in Rg3-plus-ART's effects in overcoming sorafenib resistance in hepatoma warrants further studies.

In conclusion, we for the first time found that Rg3-plus-ART overcomes sorafenib resistance in hepatoma cell and mouse models. We also found that inhibition of the Src/STAT3 pathway and modulation of the ROS/STAT3 pathway contribute to the mechanisms of action of Rg3-plus-ART. This study provides a pharmacological basis for developing Rg3-plus-ART into a novel modality for treating sorafenib-resistant hepatoma.

Declaration of competing interest

We declare that there are no conflicts of interest. Some data of this study had been used in filing a patent (202110344619.4).

Acknowledgments

This study was supported by Jilin Yatai (Group) Co., Ltd., Guangzhou MSTB (grant No.: 202009020005), Hong Kong ITC (Grant No.: ITS/092/20), Shenzhen STIC (grant No.: JCYJ20200109150719846) and STIB of Guangzhou Development District (grant No.: CY2019-005).

Appendix A. Supplementary data

Supplementary data to this article can be found online at https://doi.org/10.1016/j.jgr.2021.07.002.

References

[1] Llovet JM, Zucman-Rossi J, Eli P, Sangro B, Schwartz1 M, Sherman M, et al. Hepatocellular carcinoma. Nat Rev Dis Prim 2016;4:16018.
[2] Llovet JM, Kelley RK, Villanueva A, Singal AG, Pikarsky E, Roayaie S, et al. Hepatocellular carcinoma. Nat Rev Dis Prim 2021;7:1–28.
[3] Su D, Wu B, Shi L. Cost-effectiveness of atezolizumab plus bevacizumab *vs* sorafenib as first-line treatment of unresectable hepatocellular carcinoma. JAMA Netw Open 2021;4:1–11.
[4] Cabral LKD, Tiribelli C, Sukowati CHC. Sorafenib resistance in hepatocellular carcinoma: the relevance of genetic heterogeneity. Cancers (Basel) 2020;12:1–19.
[5] Zhao D, Zhai B, He C, Tan G, Jiang X, Pan S, et al. Upregulation of HIF-2α induced by sorafenib contributes to the resistance by activating the TGF-α/EGFR pathway in hepatocellular carcinoma cells. Cell Signal 2014;26:1030–9.
[6] Méndez-Blanco C, Fondevila F, García-Palomo A, González-Gallego J, Mauriz JL. Sorafenib resistance in hepatocarcinoma: role of hypoxia-inducible factors. Exp Mol Med 2018;50:1–9.
[7] Chen J, Duda DG. Overcoming sorafenib treatment-resistance in hepatocellular carcinoma: a future perspective at a time of rapidly changing treatment paradigms. EBioMedicine 2020;52:6–7.
[8] China Association of Chinese Medicine. Guide to TCM diagnosis and treatment of cancer. Beijing: China Press of Traditional Chinese Medicine; 2008.
[9] Li XJ, Xiao F, Xiao ML. Clinical study of Shenyi capsule combined with anlotinib in treatment of advanced non- small cell lung cancer. J Hunan Norm Univ (Med Sci). 2020;17:81–3.
[10] Tan L, Pian Y, Zheng Z. Effect of Docetaxel combined Cisplatin plus Shenyi capsule in patients advanced gastric cancer. Clin J Med Off 2019;47.

[11] Sun M, Ye Y, Xiao L, Duan X, Zhang Y, Zhang H. Anticancer effects of ginsenoside Rg3 (review). Int J Mol Med 2017;39:507–18.
[12] Meng L, Ji R, Dong X, Xu X, Xin Y, Jiang X. Antitumor activity of ginsenoside Rg3 in melanoma through downregulation of the ERK and Akt pathways. Int J Oncol 2019;54:2069–79.
[13] Jiang ZS, Yang YF, Yang YL, Zhang Y, Yue ZS, Pan ZY, et al. Ginsenoside Rg3 attenuates cisplatin resistance in lung cancer by downregulating PD-L1 and resuming immune. Biomed Pharmacother 2017;96:378–83.
[14] Zhang Y, Xu G, Zhang S, Wang D, Saravana Prabha P, Zuo Z. Antitumor research on artemisinin and its bioactive derivatives. Nat Products Bioprospect 2018;8:303–19.
[15] Markowitsch SD, Schupp P, Lauckner J, Vakhrusheva O, Slade KS, Mager R, et al. Artesunate inhibits growth of sunitinib-resistant renal cell carcinoma cells through cell cycle arrest and induction of ferroptosis. Cancers (Basel) 2020;12:1–24.
[16] Krishna S, Ganapathi S, Ster IC, Saeed MEM, Cowan M, Finlayson C, et al. A randomised, double blind, placebo-controlled pilot study of oral artesunate therapy for colorectal cancer. EBioMedicine 2015;2:82–90.
[17] von Hagens C, Walter-Sack I, Goeckenjan M, Storch-Hagenlocher B, Sertel S, Elsässer M, et al. Long-term add-on therapy (compassionate use) with oral artesunate in patients with metastatic breast cancer after participating in a phase I study (ARTIC M33/2). Phytomedicine 2019;54:140–8.
[18] He W Bin, Huang XX, Berges BK, Wang Y, An N, Su RJ, et al. Artesunate regulates neurite outgrowth inhibitor protein B receptor to overcome resistance to sorafenib in hepatocellular carcinoma cells. Front Pharmacol 2021;12:1–9.
[19] Yao X, Zhao CR, Yin H, Wang KW, Gao JJ. Synergistic antitumor activity of sorafenib and artesunate in hepatocellular carcinoma cells. Acta Pharmacol Sin 2020;41:1609–20.
[20] Xu L, Cao JP, Sun HP, Li X. Study on the anti-tumor activity of ginsenoside Rg3 combined with artesunate. China J Chinese Med 2013;28:6–7.
[21] Liu Y, Chen L, Yuan H, Guo S, Wu G. LncRNA DANCR promotes sorafenib resistance via activation of IL-6/STAT3 signaling in hepatocellular carcinoma cells. Onco Targets Ther 2020;13:1145–57.
[22] Lee S, Lee MS, Kim CT, Kim IH, Kim Y. Ginsenoside RG3 reduces lipid accumulation with AMP-activated protein kinase (AMPK) activation in HepG2 cells. Int J Mol Sci 2012;13:5729–39.
[23] Pang Y, Qin G, Wu L, Wang X, Chen T. Artesunate induces ROS-dependent apoptosis via a Bax-mediated intrinsic pathway in Huh-7 and Hep3B cells. Exp Cell Res 2016;347:251–60.
[24] Hassan Alin M, Ashton M, Kihamia CM, Mtey GJB, Björkman A. Multiple dose pharmacokinetics of oral artemisinin and comparison of its efficacy with that of oral artesunate in falciparum malaria patients. Trans R Soc Trop Med Hyg 1996;90:61–5.
[25] Liu YX, Bai JX, Li T, Fu XQ, Chen YJ, Zhu PL, et al. MiR-let-7a/f-CCR7 signaling is involved in the anti-metastatic effects of an herbal formula comprising Sophorae Flos and Lonicerae Japonicae Flos in melanoma. Phytomedicine 2019;64:153084.
[26] Tse AKW, Chen YJ, Fu XQ, Su T, Li T, Guo H, et al. Sensitization of melanoma cells to alkylating agent-induced DNA damage and cell death via orchestrating oxidative stress and IKKβ inhibition. Redox Biol 2017;11:562–76.
[27] Wu JY, Chen YJ, Bai L, Liu YX, Fu XQ, Zhu PL, et al. Chrysoeriol ameliorates TPA-induced acute skin inflammation in mice and inhibits NF-κB and STAT3 pathways. Phytomedicine 2020;68:153173.
[28] Chen YJ, Liu YX, Wu JY, Li CY, Tang MM, Bai L, et al. A two-herb formula inhibits hyperproliferation of rheumatoid arthritis fibroblast-like synoviocytes. Sci Rep 2021;11:1–9.
[29] Tovar V, Cornella H, Moeini A, Vidal S, Hoshida Y, Sia D, et al. Tumour initiating cells and IGF/FGF signalling contribute to sorafenib resistance in hepatocellular carcinoma. Gut 2017;66:530–40.
[30] Li Y, Chen G, Han Z, Cheng H, Qiao L, Li Y. IL-6/stat3 signaling contributes to sorafenib resistance in hepatocellular carcinoma through targeting cancer stem cells. Onco Targets Ther 2020;13:9721–30.
[31] Gao L, Wang X, Tang Y, Huang S, Hu CAA, Teng Y. FGF19/FGFR4 signaling contributes to the resistance of hepatocellular carcinoma to sorafenib. J Exp Clin Cancer Res 2017;36:1–10.
[32] Xu WT, Shen GN, Luo YH, Piao XJ, Wang JR, Wang H, et al. New naphthalene derivatives induce human lung cancer A549 cell apoptosis via ROS-mediated MAPKs, Akt, and STAT3 signaling pathways. Chemico-Biological Interactions 2019;304:148–57.
[33] Perillo B, Di Donato M, Pezone A, Di Zazzo E, Giovannelli P, Galasso G, et al. ROS in cancer therapy: the bright side of the moon. Exp Mol Med 2020;52:192–203.
[34] Tang W, Chen Z, Zhang W, Cheng Y, Zhang B, Wu F, et al. The mechanisms of sorafenib resistance in hepatocellular carcinoma: theoretical basis and therapeutic aspects. Signal Transduct Target Ther 2020;5:1–15.
[35] Meng J, Guo F, Xu H, Liang W, Wang C, Yang X Da. Combination therapy using Co-encapsulated resveratrol and paclitaxel in liposomes for drug resistance reversal in breast cancer cells *in vivo*. Sci Rep 2016;6:1–11.
[36] Zou L, Wang Di, Hu Y, Fu C, Li W, Dai L, et al. Drug resistance reversal in ovarian cancer cells of paclitaxel and borneol combination therapy mediated by PEG-PAMAM nanoparticles. Oncotarget 2017;8:60453–68.
[37] Dinić J, Efferth T, García-Sosa AT, Grahovac J, Padrón JM, Pajeva I, et al. Repurposing old drugs to fight multidrug resistant cancers. Drug Resist Updat 2020;52:100713.
[38] Efferth T, Oesch F. Repurposing of plant alkaloids for cancer therapy: pharmacology and toxicology. Semin Cancer Biol 2021;68:143–63.
[39] Xie L, Zeng Y, Dai Z, He W, Ke H, Lin Q, et al. Chemical and genetic inhibition of STAT3 sensitizes hepatocellular carcinoma cells to sorafenib induced cell death. Int J Biol Sci 2018;14:577–85.
[40] Tai WT, Cheng AL, Shiau CW, Liu CY, Ko CH, Lin MW, et al. Dovitinib induces apoptosis and overcomes sorafenib resistance in hepatocellular carcinoma through SHP-1-mediated inhibition of STAT3. Mol Cancer Ther 2012;11:452–63.
[41] Pelicano H, Carney D, Huang P. ROS stress in cancer cells and therapeutic implications. Drug Resist Updat 2004;7:97–110.
[42] Jiang J, Yuan Z, Sun Y, Bu Y, Li W, Fei Z. Ginsenoside Rg3 enhances the antiproliferative activity of erlotinib in pancreatic cancer cell lines by downregulation of EGFR/PI3K/Akt signaling pathway. Biomed Pharmacother 2017;96:619–25.
[43] Ma H, Yao Q, Zhang AM, Lin S, Wang XX, Wu L, et al. The effects of artesunate on the expression of EGFR and ABCG2 in A549 human lung cancer cells and a xenograft model. Molecules 2011;16:10556–69.
[44] Konkimalla V, McCubrey J, Efferth T. The role of downstream signaling pathways of the epidermal growth factor receptor for artesunates activity in cancer cells. Curr Cancer Drug Targets 2009;9:72–80.
[45] Shan X, Aziz F, Tian LL, Wang XQ, Yan Q, Liu JW. Ginsenoside Rg3-induced EGFR/MAPK pathway deactivation inhibits melanoma cell proliferation by decreasing FUT4/LeY expression. Int J Oncol 2015;46:1667–76.